New Mono- and Polynuclear Iron Silylene and Stannylene Complexes

Pierre Braunstein,*,† Michael Veith,*,‡ Joël Blin,‡ and Volker Huch‡

Laboratoire de Chimie de Coordination, UMR 7513 CNRS, Université Louis Pasteur, 4 rue Blaise Pascal, F-67070 Strasbourg Cedex, France, and Institut für Anorganische Chemie, Universität des Saarlandes, Postfach 151150, D-66041 Saarbrücken, Germany

Received June 19, 2000

The mono- and dinuclear stannylene reagents $[Sn(\mu\text{-}N^tBu)_2SiMe_2]$ (**4**) and $[Sn(O^tBu)(\mu\text{-}O^tBu)]_2$ (**6**) were reacted with the amine-stabilized bis(dimethylamino)silylene complex $[Fe\{Si(NMe_2)_2(NHMe_2)\}(CO)_4]$ (**1**), but no insertion or substitution product was detected. However, reaction of the hydridoiron silyl complex $[HFe\{Si(OMe)_3\}(CO)_3(dppm\text{-}P)]$ with **4** afforded the ion pair **7**, in which the Fe−H proton has migrated to a nitrogen atom of **4**, and with **6** by initial transfer of the Fe−H proton to a ^{t}BuO group to give the bimetallic stannylene complex $[(OC)_3\{(MeO)_3Si\}Fe(\mu\text{-dppm})Sn(O^tBu)]$ (**8**), in which the Sn atom has a distorted-trigonal-pyramidal coordination. The tin(II) compound **6** also reacted with $[Fe_2(CO)_9]$ to afford the new tin−iron complex $[Fe(CO)_4Sn(O^tBu)(\mu\text{-}O^tBu)]_2$ (**9**), which contains a central Sn_2O_2 planar core. In contrast, reaction of **4** with $[Fe_2(CO)_9]$ yielded $[(OC)_4Fe\{\mu\text{-}Sn(\mu\text{-}N^tBu)_2SiMe_2\}]_2$ (**10**), which contains a central, planar Sn_2Fe_2 core. All compounds were characterized by multinuclear NMR spectroscopy, and the molecular structures of **1**, **8**·THF, and **9** (triclinic (**9a**) and monoclinic (**9b**) forms) were determined by X-ray diffraction.

Introduction

The rich chemistry of silyl- and silylenemetal complexes has generated a number of issues of fundamental interest which, together with the involvement of such complexes in important catalytic processes, account for the increasing interest in these classes of molecules.[1] Striking similarities and differences are observed with the corresponding alkyl and carbene complexes and, likewise, with stannyl and stannylene metal complexes, respectively.[2] The first thermally stable free silylene, the bis(amino)silylene $:Si[N(^tBu)CH{=}CHN(^tBu)]$, was prepared in 1994 with the help of additional aromatic stabilization,[3] whereas the X-ray structure of the crystalline bis(amino)silylene $:Si[\{N(CH_2{}^tBu)\}_2C_6H_4\text{-}1,2]$ was reported in 1995.[4] Although the first metal−silylene complex was reported in 1977,[5] structural characterization by X-ray diffraction methods of stable mononuclear silylene complexes was only achieved in 1987−1988.[6] The role of surface-bound silylenes in the direct process for the selective heterogeneously catalyzed synthesis of $SiMe_2Cl_2$ has been confirmed by trapping experiments with butadiene.[7] The first stannylenemetal complex, $[Fe(Sn^tBu_2)(CO)_4]$,[8] was reported by Hieber in 1957, and this opened up a very dynamic field of research.[2,9] Relatively small changes in the ligands or substituents used are often sufficient to induce very different structural or chemical properties.[10] Whereas oxidative addition of $HSi(OMe)_3$ to $[Fe(CO)_5]$ yields the hydridosilyl complex *cis*-$[HFe\{Si(OMe)_3\}(CO)_4]$, the corresponding

† Université Louis Pasteur. E-mail: braunst@chimie.u-strasbg.fr.
‡ Universität des Saarlandes.

(1) (a) Mackay, K. M.; Nicholson, B. K. In *Comprehensive Organometallic Chemistry*; Wilkinson, G., Stone, F. G. A., Abel, E. W., Eds.; Pergamon Press: Oxford, England, 1982; Chapter 43. (b) Ojima, I. In *The Chemistry of Organic Silicon Compounds*; Patai, S., Rappoport, Z., Eds.; Wiley: Chichester, U.K., 1989; p 1479. (c) Tilley, T. D. In *The Silicon-Heteroatom Bond*; Patai, S., Rappoport, Z., Eds.; Wiley: New York, 1991; pp 245, 309. (d) Zybill, C. *Top. Curr. Chem.* **1991**, *160*, 1. (e) Marciniec, B.; Gulinski, J.; Urbaniak, W.; Kornetka, Z. W. In *Comprehensive Handbook of Hydrosilylation*; Marciniec, B., Ed.; Pergamon Press: Tokyo, 1992. (f) Corriu, R. J. P.; Lanneau, G. F.; Chauhan, B. S. P. *Organometallics* **1993**, *12*, 2001. (g) Zybill, C.; Handwecker, H.; Friedrich, H. *Adv. Organomet. Chem.* **1994**, *36*, 229. (h) Braunstein, P.; Knorr, M. *J. Organomet. Chem.* **1995**, *500*, 21. (i) Lewis, L. N. In *Catalysis by Di- and Polynuclear Metal Cluster Complexes*; Adams, R. D., Cotton, F. A., Eds.; Wiley-VCH: New York, 1998; p 373. (j) Braunstein, P.; Knorr, M.; Stern, C. *Coord. Chem. Rev.* **1998**, *178−180*, 903. (k) Corey, J. Y.; Braddock-Wilking, J. *Chem. Rev.* **1999**, *99*, 175. (l) Bender, R.; Braunstein, P.; Bouaoud, S.-E.; Merabet, N.; Rouag, D.; Zanello, P.; Fontani, M. *New J. Chem.* **1999**, *23*, 1045. (m) Haaf, M.; Schmedake, T. A.; West, R. *Acc. Chem. Res.* **2000**, *33*, 704. See also the references cited in these papers.

(2) Petz, W. *Chem. Rev.* **1986**, *86*, 1019.

(3) (a) Denk, M.; Lennon, R.; Hayashi, R.; West, R.; Belayakov, A. V.; Verne, H. P.; Haaland, A.; Wagner, M.; Metzler, N. *J. Am. Chem. Soc.* **1994**, *116*, 2691. (b) Heinemann, C.; Müller, T.; Apeloig, Y.; Schwarz, H. *J. Am. Chem. Soc.* **1996**, *118*, 2023. (c) Boehme, C.; Frenking, G. *J. Am. Chem. Soc.* **1996**, *118*, 2039. (d) West, R.; Buffy, J. J.; Haaf, M.; Müller, T.; Gehrhus, B.; Lappert, M. F.; Apeloig, Y. *J. Am. Chem. Soc.* **1998**, *120*, 1639.

(4) Gerhus, B.; Lappert, M. F.; Heinicke, J.; Boese, R.; Bläser, D. *J. Chem. Soc., Chem. Commun.* **1995**, 1931.

(5) Schmid, G.; Welz, E. *Angew. Chem., Int. Ed. Engl.* **1977**, *16*, 785.

(6) (a) Straus, D. A.; Tilley, T. D.; Rheingold, A. L.; Geib, S. J. *J. Am. Chem. Soc.* **1987**, *109*, 5872. (b) Zybill, C.; Müller, G. *Angew. Chem., Int. Ed. Engl.* **1987**, *26*, 669. (c) Zybill, C.; Müller, G. *Organometallics* **1988**, *7*, 1368. (d) Zybill, C.; Wilkinson, D. L.; Leis, C.; Müller, G. *Angew. Chem., Int. Ed. Engl.* **1988**, *27*, 583. (e) Ueno, K.; Tobita, H.; Shimoi, M.; Ogino, H. *J. Am. Chem. Soc.* **1988**, *110*, 4092. (f) Zybill, C.; Wilkinson, D. L.; Leis, C.; Müller, G. *Angew. Chem., Int. Ed. Engl.* **1989**, *28*, 203. (f) Leis, C.; Wilkinson, D. L.; Handwerker, H.; Zybill, C. *Organometallics* **1992**, *11*, 514. (g) Handwerker, H.; Leis, C.; Gamper, S.; Zybill, C. *Inorg. Chim. Acta* **1992**, *198−200*, 763.

(7) Clarke, M. P.; Davidson, I. M. T. *J. Organomet. Chem.* **1991**, *408*, 149.

(8) Hieber, W.; Breu, R. *Chem. Ber.* **1957**, *90*, 1270.

(9) (a) Holt, M. S.; Wilson, W. L.; Nelson, J. H. *Chem. Rev.* **1989**, *89*, 11. (b) Braunstein, P.; Morise, X. *Chem. Rev.* **2000**, *10*, 3541.

(10) Veith, M. In *Metal Clusters in Chemistry*; Braunstein, P., Oro, L. A., Raithby, P. R., Eds.; Wiley-VCH: Weinheim, Germany, 1999; Vol. 1, pp 73−90.

10.1021/om000515z CCC: $20.00
Publication on Web 01/24/2001

reaction with $HSi(NMe_2)_3$ affords instead the amine-stabilized bis(dimethylamino)silylene complex $[Fe\{Si(NMe_2)_2(NHMe_2)\}(CO)_4]$ (**1**).[11] This contrasting behavior is explained by the more favorable migration of the acidic proton of the suggested hydrido tris(dimethylamino)silyl intermediate to the nitrogen atom of an amino substituent, which is more basic than the methoxy group of the $Si(OMe)_3$ ligand (eq 1).[1j,12]

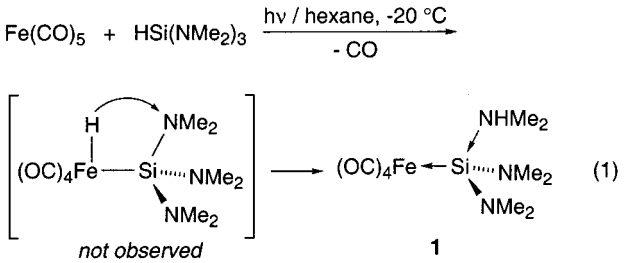

(1)

When $[Fe(CO)_4\{P(OMe)_3\}]$ was used in place of $[Fe(CO)_5]$, the related base-stabilized silylene complex $[Fe\{Si(OMe)_2(NHMe_2)\}(CO)_3\{P(NMe_2)_2(OMe)\}]$ (**2a**) was isolated in 30−40% yield.[13]

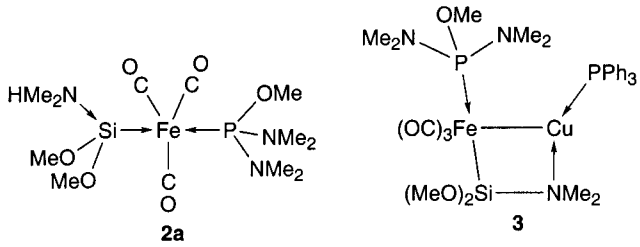

This complex resulted from a selective metal-promoted OMe/NMe_2 substituent exchange between phosphorus and silicon. It was obtained in 80% yield by a cross-experiment consisting of the reaction of $[Fe(CO)_4\{P(NMe_2)_3\}]$ with $HSi(OMe)_3$. The competing oxophilicity of the phosphorus and silicon centers triggers these remarkable and selective rearrangements. Deprotonation of **2a** with excess KH afforded the metalate complex $K[Fe\{Si(OMe)_2(NMe_2)\}(CO)_3\{P(OMe)(NMe_2)_2\}]$, the metal-centered basicity of which allowed the synthesis of **3**, the first bimetallic complex with an aminosilyl bridging ligand.[13]

In contrast, the reaction of **2a** with the stannylene reagent $[Sn(\mu\text{-}N^tBu)_2SiMe_2]$ (**4**), a rare example of a monomeric stannylene compound in the solid state,[14] occurred by insertion of the latter into the N−H bond of **2a**,**b** to give **5a**,**b**, respectively, a novel type of base-stabilized silylene stannylene complex (eq 2).[15]

Here we report further studies on the synthesis and reactivity of related silylene and stannylene compounds.

Results and Discussion

As a ligand, the stannylene **4** displays a versatile behavior toward mononuclear metal complexes[16−19] as well as bimetallic Fe−Pd and Fe−Pt complexes.[20] The result shown in eq 2 raised the question whether the

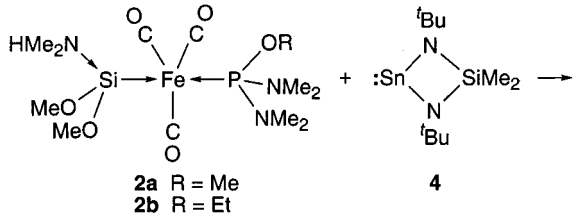

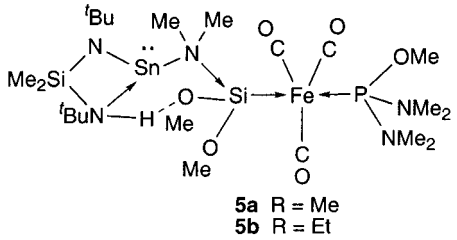

(2)

reaction of **4** with **1** could possibly occur by replacement of the amine ligand or of a CO ligand or by insertion into its NH bond, as observed with **2a**,**b**. Progressive addition of **4** to a toluene solution of **1** even at −30 °C resulted in a rapid darkening of the reaction mixture and the formation of numerous products (^1H and $^{29}Si\{^1H\}$ NMR monitoring) which could not be identified. Varying the solvent or the reaction temperature led to similar results.

We then turned our attention from the bis(amino)-stannylene to the dimeric bis(alkoxo)stannylene reagent $[Sn(O^tBu)(\mu\text{-}O^tBu)]_2$ (**6**), which crystallizes in the form of a dimer,[21] and reacted it with **1** in toluene at −20 °C. Very rapid darkening of the reaction mixture occurred around room temperature, and monitoring by ^1H, $^{13}C\{^1H\}$, and $^{29}Si\{^1H\}$ NMR clearly indicated the presence of numerous species that could not be identified. In the course of one of these experiments, the temperature of the reaction mixture was raised from −20 to −5 °C and the solution was kept at this temperature for a few days. Brown crystals formed, which were characterized in solution by ^1H and $^{29}Si\{^1H\}$ NMR spectroscopy and found to be unreacted **1**. Since they were suitable for X-ray diffraction, the crystal structure was determined, as no direct structural information had been available before.[11] A view of the molecular structure is shown in Figure 1, and selected bond distances and angles are given in Table 1.

In contrast to the ethoxy derivative **2b**, which crystallizes as pseudo-dimers owing to intermolecular NH···O bonding,[11] **1** exists as monomeric units in the solid state. The coordination geometry around the Fe center is trigonal bipyramidal, with the silicon ligand in an apical position. The iron−silicon distance of 2.292(1) Å is longer than in **2b** (2.218(2) Å) but comparable to that

(11) Bodensieck, U.; Braunstein, P.; Deck, W.; Faure, T.; Knorr, M.; Stern, C. *Angew. Chem., Int. Ed. Engl.* **1994**, *33*, 2440.
(12) Schmid, G.; Welz, E. *Angew. Chem., Int. Ed. Engl.* **1977**, *16*, 785.
(13) Braunstein, P.; Stern, C.; Strohmann, C.; Tong, N. *J. Chem. Soc., Chem. Commun.* **1996**, 2237.
(14) Veith, M.; *Z. Naturforsch.* **1978**, *33B*, 7.
(15) Braunstein, P.; Huch, V.; Stern, C.; Veith, M. *J. Chem. Soc., Chem. Commun.* **1996**, 2041.
(16) Veith, M.; Lange, H.; Bräuer, K.; Bachmann, R. *J. Organomet. Chem.* **1981**, *216*, 377.
(17) (a) Veith, M.; Stahl, L.; Huch, V. *J. Chem. Soc., Chem. Commun.* **1990**, 359. (b) Veith, M.; Stahl, L. *Angew. Chem., Int. Ed. Engl.* **1993**, *32*, 106.
(18) Veith, M.; Stahl, L.; Huch, V. *Organometallics* **1993**, *12*, 1914.
(19) Veith, M.; Müller, A.; Stahl, L.; Nötzel, M.; Jarczyk, M.; Huch, V. *Inorg. Chem.* **1996**, *35*, 3848.
(20) Knorr, M.; Hallauer, E.; Huch, V.; Veith, M.; Braunstein, P. *Organometallics* **1996**, *15*, 3868.
(21) Veith, M.; Hobein, P.; Rösler, R. *Z. Naturforsch.* **1989**, *44B*, 1067.

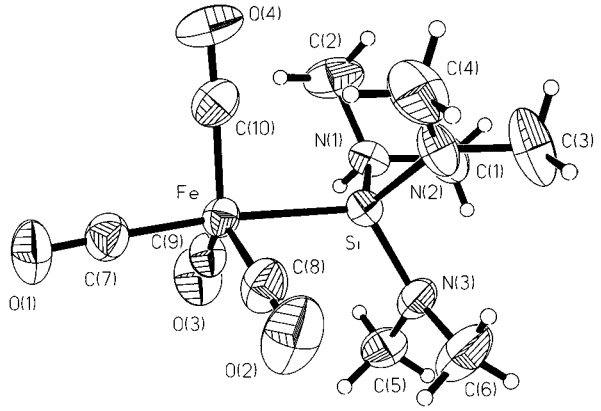

Figure 1. ORTEP view of the molecular structure of [Fe{Si(NMe$_2$)$_2$(NHMe$_2$)}(CO)$_4$] (**1**). Thermal ellipsoids are drawn at 30% probability.

Table 1. Selected Bond Distances (Å) and Angles (deg) for [Fe{Si(NMe$_2$)$_2$(NHMe$_2$)}(CO)$_4$] (1)

Fe−C(7)	1.787(4)	N(1)−C(2)	1.487(4)
Fe−C(8)	1.767(4)	N(2)−C(3)	1.458(5)
Fe−C(9)	1.751(4)	N(2)−C(4)	1.463(5)
Fe−C(10)	1.765(4)	N(3)−C(5)	1.458(4)
Fe−Si	2.292(1)	N(3)−C(6)	1.457(5)
Si−N(1)	1.942(3)	O(1)−C(7)	1.142(4)
Si−N(2)	1.701(3)	O(2)−C(8)	1.146(4)
Si−N(3)	1.731(3)	O(3)−C(9)	1.151(4)
N(1)−C(1)	1.490(5)	O(4)−C(10)	1.154(4)
C(9)−Fe−C(10)	117.6(2)	N(1)−Si−Fe	109.5(1)
C(9)−Fe−C(8)	122.7(2)	C(2)−N(1)−C(1)	109.5(3)
C(10)−Fe−C(8)	118.5(2)	C(2)−N(1)−Si	113.4(2)
C(9)−Fe−C(7)	93.6(2)	C(1)−N(1)−Si	116.6(2)
C(10)−Fe−C(7)	94.7(2)	C(3)−N(2)−C(4)	110.7(3)
C(8)−Fe−C(7)	93.0(2)	C(3)−N(2)−Si	124.1(3)
C(9)−Fe−Si	86.8(1)	C(4)−N(2)−Si	125.1(3)
C(10)−Fe−Si	90.8(1)	C(6)−N(3)−C(5)	111.5(3)
C(8)−Fe−Si	81.5(1)	C(6)−N(3)−Si	118.7(3)
C(7)−Fe−Si	173.6(1)	C(5)−N(3)−Si	121.3(2)
N(2)−Si−N(3)	105.7(1)	O(1)−C(7)−Fe	178.2(3)
N(2)−Si−N(1)	104.4(1)	O(2)−C(8)−Fe	178.1(3)
N(3)−Si−N(1)	96.3(1)	O(3)−C(9)−Fe	178.1(3)
N(2)−Si−Fe	118.7(1)	O(4)−C(10)−Fe	178.1(3)
N(3)−Si−Fe	118.9(1)		

found in [Fe{SiMe$_2$·HMPA}(CO)$_4$] (2.280(1) Å).[1d] When the NHMe$_2$ ligand is ignored, the sum of the three angles around the Si atom amounts to 343.41°, which indicates noticeable deformation away from an sp^2-type hybridization. The Si−N(1) distance (1.942(3) Å) is remarkably longer than the other two Si−N distances (Si−N(2) = 1.701(3) Å and Si−N(3) = 1.731(3) Å), which may be explained by the higher coordination number of 4 at N(1) compared to 3 at N(2) and N(3). Accordingly, the Si−N(1) distance is longer than a normal single bond (1.73−1.79 Å) and comparable to the Si−NHMe$_2$ distance in **2b** (1.916(5) Å). The much shorter Si−N(2) and Si−N(3) distances and the planar coordination geometry of these nitrogen atoms indicate sp^2 hybridization, which could favor N−Si p$\pi \rightarrow$ dπ interactions.

Since the reactions between **1** and the stannylene reagents **4** or **6** failed to give well-identified compounds, we turned our attention to the hydridoiron silyl complex [HFe{Si(OMe)$_3$}(CO)$_3$(dppm-*P*)], which has a rich chemistry.[1j] Addition of a stoichiometric amount of **4** to a THF solution of the hydrido complex induced a rapid darkening of the solution. After the reaction mixture was stirred for 1 h, the ^{31}P{^{1}H} NMR spectrum contained two doublets at δ −24 and 74 (^2J(PP) = 85 Hz), assigned to the uncoordinated and Fe-bound atoms of the metalate [Fe{Si(OMe)$_3$}(CO)$_3$(dppm-*P*)]$^-$, respectively. The ^{119}Sn{^{1}H} multiplet resonance at δ −496.9 indicated that Sn(II) was still present in the product (cf. δ 636 for **4**). Consistent with previous findings showing that **4** readily adds a proton on one of the nitrogen atoms,[22] we suggest that the reaction occurred according to eq 3, although the product **7** decomposed rapidly in the solid state and could not be further characterized.

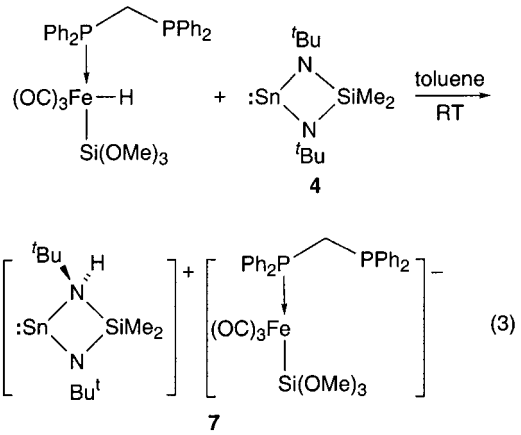

The reaction of [HFe{Si(OMe)$_3$}(CO)$_3$(dppm-*P*)] in THF with **6** instead of **4** afforded a red solution which darkened very rapidly. The ^{31}P{^{1}H} NMR spectrum of the final solution contained two doublets with $^{117/119}$Sn satellites. The resonance at δ 63 is assigned to the Fe-bound P atom and shows coupling constants of 132 Hz with the other P nucleus, 61 Hz with tin, and 24 Hz with silicon. The other resonance, at δ −15, shows ^1J(PSn) coupling constants of 703 Hz with ^{119}Sn and 672 Hz with ^{117}Sn, whose ratio is as expected: $\gamma(^{119}\text{Sn})/\gamma(^{117}\text{Sn}) = 1.046$. The ^{119}Sn{^{1}H} resonance appears as a doublet of doublets at δ 404.5 and, likewise, the ^{29}Si{^{1}H} resonance at δ 5. These data are consistent with a dppm-bridged Fe−Sn complex. Since small, dark red crystals of **8** formed at −5 °C, they could be analyzed by X-ray diffraction. This established the structure of this new complex (Figure 2), and selected bond distances and angles are given in Table 2.

The complex [(OC)$_3${(MeO)$_3$Si}Fe(μ-dppm)Sn(O^{t}Bu)] (**8**) crystallizes with one molecule of THF per formula unit. The THF molecules do not interact with the acidic centers of the molecule but serve to optimize crystal packing. The Fe atom is in a slightly distorted octahedral environment with three coplanar CO ligands, a P atom and a Si atom in mutually trans positions, and the Sn atom. The second P atom is coordinated to the Sn atom, which has a distorted-trigonal-pyramidal coordination with interligand angles of 96.9(3)° (Fe(1)−Sn(1)−O(4)), 86.73(8)° (Fe(1)−Sn(1)−P(2)), and 78.1(3)° (P(2)−Sn(1)−O(4)). This stereogenic tin center is typical for the formal oxidation state II, with the lone pair occupying the apical position.[23] Note that the latter is

(22) (a) Veith, M. *Angew. Chem., Int. Ed. Engl.* **1987**, *26*, 1. (b) Veith, M.; Töllner, F. *J. Organomet. Chem.* **1983**, *246*, 219. (c) Veith, M.; Olbrich, M.; Shihua, W.; Huch, V. *J. Chem. Soc., Dalton Trans.* **1996**, 161.

(23) Veith, M.; Recktenwald, T. *Top. Curr. Chem.* **1982**, *104*, 1.

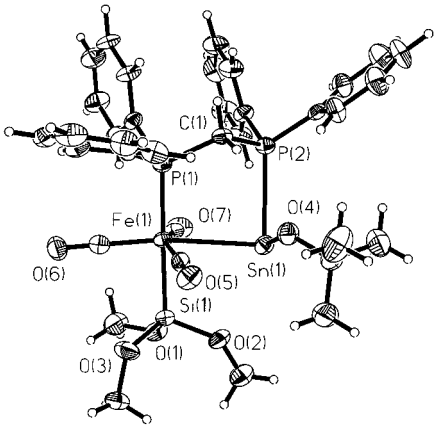

Figure 2. ORTEP view of the molecular structure of $[(OC)_3\{(MeO)_3Si\}Fe(\mu\text{-dppm})Sn(O^tBu)]\cdot THF$ (**8**·THF). Thermal ellipsoids are drawn at 30% probability.

Table 2. Selected Bond Distances (Å) and Angles (deg) for $[(OC)_3\{(MeO)_3Si\}Fe(\mu\text{-dppm})Sn(O^tBu)]$ (8)

Sn(1)−O(4)	2.044(8)	Si(1)−O(3)	1.631(9)
Sn(1)−P(2)	2.827(3)	Si(1)−O(2)	1.636(9)
Sn(1)−Fe(1)	2.854(2)	Si(1)−O(1)	1.647(8)
Fe(1)−C(34)	1.76(2)	O(1)−C(26)	1.39(2)
Fe(1)−C(33)	1.77(1)	O(2)−C(27)	1.38(2)
Fe(1)−C(35)	1.77(1)	O(3)−C(28)	1.41(2)
Fe(1)−P(1)	2.210(4)	O(4)−C(29)	1.44(2)
Fe(1)−Si(1)	2.267(4)	O(5)−C(33)	1.16(1)
P(1)−C(8)	1.82(1)	O(6)−C(34)	1.16(1)
P(1)−C(1)	1.83(1)	O(7)−C(35)	1.16(1)
P(1)−C(2)	1.86(1)	C(29)−C(31)	1.49(2)
P(2)−C(20)	1.79(1)	C(29)−C(32)	1.53(2)
P(2)−C(14)	1.82(1)	C(29)−C(30)	1.53(2)
P(2)−C(1)	1.84(1)		
O(4)−Sn(1)−P(2)	78.1(3)	C(1)−P(2)−Sn(1)	97.5(4)
O(4)−Sn(1)−Fe(1)	96.9(3)	O(3)−Si(1)−O(1)	106.8(5)
P(2)−Sn(1)−Fe(1)	86.73(8)	O(3)−Si(1)−O(2)	108.3(5)
C(34)−Fe(1)−C(33)	101.6(5)	O(2)−Si(1)−O(1)	101.5(5)
C(34)−Fe(1)−C(35)	103.2(5)	O(1)−Si(1)−Fe(1)	119.1(3)
C(33)−Fe(1)−C(35)	151.5(6)	O(2)−Si(1)−Fe(1)	109.6(3)
C(34)−Fe(1)−P(1)	92.7(4)	O(3)−Si(1)−Fe(1)	110.8(4)
C(33)−Fe(1)−P(1)	91.2(4)	C(26)−O(1)−Si(1)	125.4(9)
C(35)−Fe(1)−P(1)	101.4(4)	C(27)−O(2)−Si(1)	129.4(9)
C(34)−Fe(1)−Si(1)	87.9(4)	C(28)−O(3)−Si(1)	125.9(9)
C(33)−Fe(1)−Si(1)	82.1(4)	C(29)−O(4)−Sn(1)	121.5(8)
C(35)−Fe(1)−Si(1)	84.9(4)	P(1)−C(1)−P(2)	113.9(6)
P(1)−Fe(1)−Si(1)	173.3(1)	O(4)−C(29)−C(30)	105(1)
C(34)−Fe(1)−Sn(1)	171.0(4)	O(4)−C(29)−C(31)	111(1)
C(33)−Fe(1)−Sn(1)	80.2(4)	O(4)−C(29)−C(32)	111(1)
C(35)−Fe(1)−Sn(1)	73.1(4)	O(5)−C(33)−Fe(1)	176(1)
P(1)−Fe(1)−Sn(1)	96.1(1)	O(6)−C(34)−Fe(1)	178(1)
Si(1)−Fe(1)−Sn(1)	83.6(1)	O(7)−C(35)−Fe(1)	177(1)
C(1)−P(1)−Fe(1)	116.8(4)		

not involved in bonding to iron. As in other trigonal pyramidally coordinated tin(II) compounds, the tin atom is not electrophilic, and this explains why the O(2)···Sn(1) separation of 2.914(8) Å is too long to represent a bonding interaction. The Si atom is in an almost regular tetrahedral environment. The Fe−Sn distance (2.854(2) Å) is relatively long when compared to those in other Fe−Sn complexes,[24] and this underlines our assumption that the Sn−Fe bond involves an Sn(II) oxidation state, as bonding to Sn(II) leads to longer σ-bonds compared to Sn(IV) because of less polarized orbital character in the bonding. The P(2)−Sn(1) distance of 2.827(3) Å indicates a rather weak interaction; however, it is sufficient to stabilize this new metallostannylene complex in a monomeric form. This distance is, however, shorter than in the Fe−Sn(IV) complex *mer,cis*-$[Fe(CO)_3(dppm)(SnClPh_2)_2]$ (3.140(2) Å).[25]

The reaction leading to **8** (eq 4) can be understood as being initiated by a proton transfer from Fe to a ^{t}BuO group, resulting in the thermodynamically favorable formation of ^{t}BuOH and of an Fe−Sn bond in a five-membered ring. Formally, the $[Sn^{II}-O^tBu]^+$ moiety in

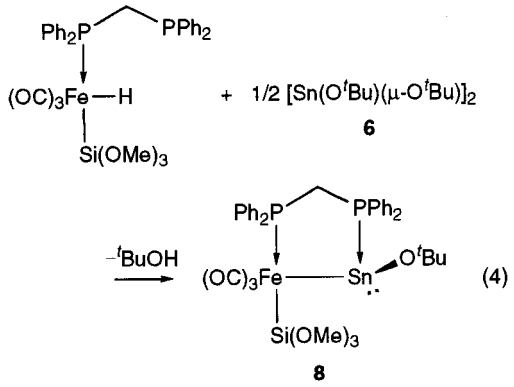

8 may be viewed as replacing the proton in $[HFe\{Si(OMe)_3\}(CO)_3(dppm\text{-}P)]$.

If the stannylene **6** were to be reacted with an iron complex that does not contain an acidic hydrogen, elimination of ^{t}BuOH should not occur. This was indeed the case in the reaction of **6** with $[Fe_2(CO)_9]$, which afforded the new tin−iron complex $[Fe(CO)_4Sn(O^tBu)(\mu\text{-}O^tBu)]_2$ **9** (eq 5).

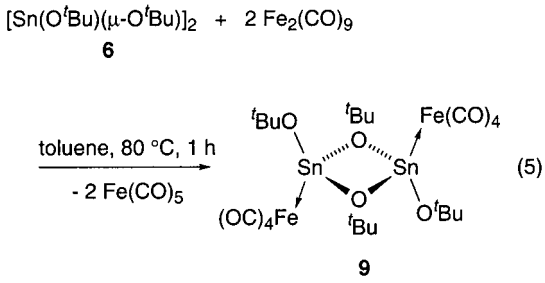

Crystals obtained from a toluene solution at −5 °C were triclinic with $Z = 1$ (**9a**), whereas those grown at room temperature were monoclinic with $Z = 2$ (**9b**). In both cases, the molecules, which only differ by the mutual orientation of the ^{t}Bu and CO groups, have crystallographically imposed centrosymmetry (Figures 3 and 4). The bonding parameters for both structures are therefore very similar (see Tables 3 and 4, respectively), and only the structure of **9a** will be briefly discussed. The Sn_2O_2 ring is thus perfectly planar and forms a nearly perfect rhombus, since the Sn(1)−O(1) and Sn(1)−O(1′) distances are almost identical (2.094(3) and 2.099(3) Å, respectively). These values are shorter than in the precursor complex **6**, as also observed in the related complex $[Fe\{Sn(OAr)_2\}(CO)_4]$.[26]

(24) (a) Braunstein, P.; Charles, C.; Adams, R. D.; Layland, R. *J. Cluster Sci.* **1996**, *7*, 145. (b) Braunstein, P.; Charles, C.; Tiripicchio, A.; Ugozzoli, F. *J. Chem. Soc., Dalton Trans.* **1996**, 4365. (c) Braunstein, P.; Charles, C.; Kickelbick, G.; Schubert, U. *J. Chem. Soc., Chem. Commun.* **1997**, 1911. (d) Braunstein, P.; Charles, C.; Kickelbick, G.; Schubert, U. *J. Chem. Soc., Chem. Commun.* **1997**, 2093.

(25) Braunstein, P.; Knorr, M.; Strampfer, M.; DeCian, A.; Fischer, J. *J. Chem. Soc., Dalton Trans.* **1994**, 117.

(26) Hitchcock, P. B.; Lappert, M. F.; Thomas, S. A.; Thorne, A. J.; Carty, A. J.; Taylor, N. J. *J. Organomet. Chem.* **1986**, *315*, 27.

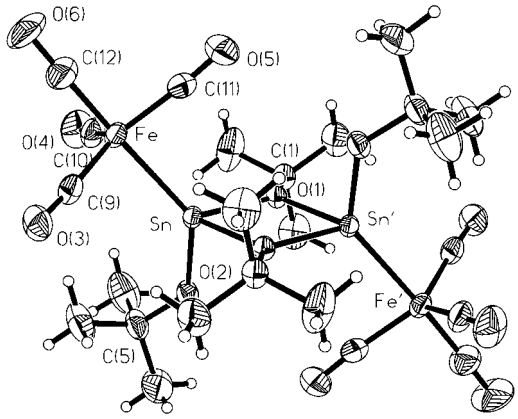

Figure 3. ORTEP view of the molecular structure of [Fe(CO)$_4$Sn(O^{t}Bu)(μ-O^{t}Bu)]$_2$ (**9a**; triclinic). Thermal ellipsoids are drawn at 30% probability.

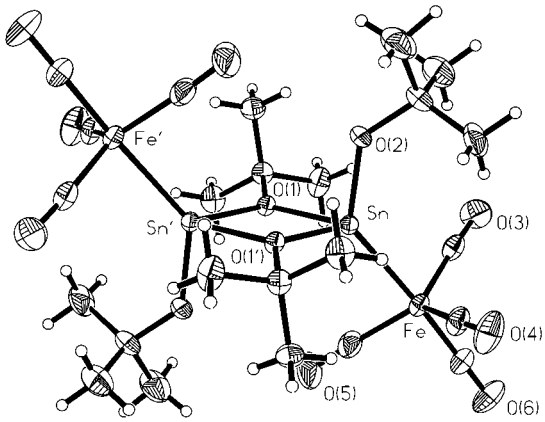

Figure 4. ORTEP view of the molecular structure of [Fe(CO)$_4$Sn(O^{t}Bu)(μ-O^{t}Bu)]$_2$ (**9b**; monoclinic). Thermal ellipsoids are drawn at 30% probability.

Table 3. Selected Bond Distances (Å) and Angles for [Fe(CO)$_4$Sn(O^{t}Bu)(μ-O^{t}Bu)]$_2$ (9a)[a]

Sn(1)−O(1)	2.094(3)	O(3)−C(9)	1.132(6)
Sn(1)−O(1)′	2.099(3)	O(4)−C(10)	1.143(7)
Sn(1)−O(2)	1.936(3)	O(5)−C(11)	1.137(6)
Sn(1)−Fe(2)	2.4678(9)	O(6)−C(12)	1.151(7)
Fe(2)−C(9)	1.790(6)	C(1)−C(2)	1.542(8)
Fe(2)−C(10)	1.775(6)	C(1)−C(3)	1.485(8)
Fe(2)−C(11)	1.785(6)	C(1)−C(4)	1.480(8)
Fe(2)−C(12)	1.752(6)	C(5)−C(6)	1.480(8)
O(1)−C(1)	1.466(5)	C(5)−C(7)	1.485(9)
O(2)−C(5)	1.442(6)	C(5)−C(8)	1.54(1)

O(2)−Sn(1)−O(1)	93.0(1)	O(2)−Sn(1)−O(1)′	93.45(13)
O(1)−Sn(1)−O(1)′	73.4(1)	O(2)−Sn(1)−Fe(2)	135.0(1)
O(1)−Sn(1)−Fe(2)	121.83(8)	O(1)′−Sn(1)−Fe(2)	121.68(8)
C(12)−Fe(2)−C(10)	92.4(3)	C(12)−Fe(2)−C(11)	89.5(3)
C(10)−Fe(2)−C(11)	117.6(3)	C(12)−Fe(2)−C(9)	89.1(3)
C(10)−Fe(2)−C(9)	115.5(2)	C(11)−Fe(2)−C(9)	126.9(2)
C(12)−Fe(2)−Sn(1)	175.1(3)	C(10)−Fe(2)−Sn(1)	92.4(2)
C(11)−Fe(2)−Sn(1)	87.48(16)	C(9)−Fe(2)−Sn(1)	89.6(2)
C(1)−O(1)−Sn(1)	127.2(2)	C(1)−O(1)−Sn(1)′	125.5(2)
Sn(1)−O(1)−Sn(1)′	106.6(2)	C(5)−O(2)−Sn(1)	130.7(3)
O(1)−C(1)−C(4)	108.8(4)	O(1)−C(1)−C(3)	108.8(4)
C(4)−C(1)−C(3)	114.0(5)	O(1)−C(1)−C(2)	104.7(4)
C(4)−C(1)−C(2)	110.5(5)	C(3)−C(1)−C(2)	109.7(5)
O(2)−C(5)−C(6)	112.8(4)	O(2)−C(5)−C(7)	106.1(5)
C(6)−C(5)−C(7)	112.9(7)	O(2)−C(5)−C(8)	107.0(5)
C(6)−C(5)−C(8)	107.7(6)	C(7)−C(5)−C(8)	110.2(7)
O(3)−C(9)−Fe(2)	176.3(5)	O(4)−C(10)−Fe(2)	176.6(5)
O(5)−C(11)−Fe(2)	175.5(5)	O(6)−C(12)−Fe(2)	178.3(8)

[a] Symmetry transformations used to generate equivalent primed atoms: $-x, -y + 2, -z + 1$.

The phenomenon of shrinkage of adjacent bond lengths when a tin(II) center is coordinated to transition metals is well established[19] and can be explained by an electron transfer to the transition metal. The carbon atom C(1) is coplanar with the Sn_2O_2 unit, since the coordination geometry of the sp^2-hybridized O(1) is almost perfectly planar. The coordination geometry around iron is trigonal bipyramidal with the Fe(CO)$_4$ fragment being at a distance of 2.4678(9) Å to the tin center. The value for this bond is shorter than in other Fe−Sn complexes involving a tetracoordinate tin atom.[24b] This indicates a strong Fe−Sn interaction, the stannylene ligand behaving as a strong σ-donor, weak π-acceptor ligand.[27] In solution, the bridging and terminal ^{t}BuO groups are in fast exchange on the NMR time scale, since they only give rise to a singlet at room temperature in ^{1}H and ^{13}C{^{1}H} NMR spectroscopy.

It is interesting to compare the reaction between **6** and [Fe$_2$(CO)$_9$] with that observed between **4** and [Fe$_2$(CO)$_9$] (eq 6), since it afforded [(OC)$_4$Fe{μ-Sn(μ-N^{t}Bu)$_2$SiMe$_2$}]$_2$ (**10**), which contains a central Fe_2Sn_2 core.[28] This reaction required, nevertheless, much harsher

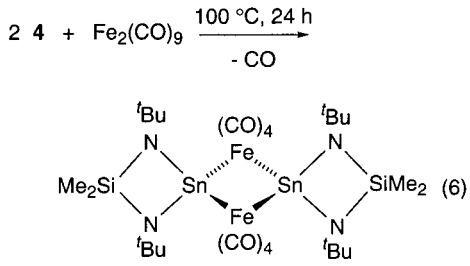

conditions (100 °C, 24 h). Obviously, the propensity to retain the [Sn(O^{t}Bu)(μ-O^{t}Bu)]$_2$ dimeric unit in compound **9** appears to be greater than the tendency to adopt a structure of type **10** with bridging Fe(CO)$_4$ units.

Experimental Section

All reactions and manipulations were carried out under an inert atmosphere of purified nitrogen using standard Schlenk tube techniques. Solvents were dried and distilled under nitrogen before use: hexane and toluene over sodium, tetrahydrofuran and diethyl ether over sodium−benzophenone, dichloromethane over phosphorus pentoxide. Nitrogen (Air liquide, R-grade) was passed through BASF R3-11 catalyst and molecular sieves columns to remove residual oxygen and water. Elemental C, H, and N analyses were performed with a CHN-900 instrument from LECO Corp., St. Joseph, MI. Infrared spectra were recorded on an IFS 66 Bruker FT-IR spectrometer. The ^{1}H and ^{31}P{^{1}H} NMR spectra were recorded at 300.1 and 121.5 MHz, respectively, on a Bruker AM300 instrument and the ^{119}Sn NMR spectra at 149 MHz on a Bruker AC400 instrument. Some samples have been analyzed on a Bruker AC200P instrument, at 200.13 MHz (^{1}H), 50.32 MHz (^{13}C), 39.76 MHz (^{29}Si), 81.0 MHz (^{31}P), and 74.68 MHz (^{119}Sn).

The compounds [Fe{Si(NMe$_2$)$_2$(NHMe$_2$)}(CO)$_4$] (**1**),[11] [Sn(μ-N^{t}Bu)$_2$SiMe$_2$] (**4**),[29] and [Sn(O^{t}Bu)(μ-O^{t}Bu)]$_2$ (**6**)[21] were prepared as reported in the literature.

(27) Davies, A. G. *Organotin Chemistry*; VCH: Weinheim, Germany, 1997; p 262.
(28) Olbrich, M. Doctoral Thesis, Saarbrücken University, 1996.
(29) Veith, M. *Angew. Chem., Int. Ed. Engl.* **1975**, *14*, 263.

Table 4. Selected Bond Distances (Å) and Angles (deg) for $[Fe(CO)_4Sn(O^tBu)(\mu\text{-}O^tBu)]_2$ (9b)[a]

Sn(1)−O(2)	1.943(3)	O(2)−C(5)	1.449(6)
Sn(1)−O(1)′	2.088(3)	O(3)−C(9)	1.149(6)
Sn(1)−O(1)	2.097(3)	O(4)−C(10)	1.155(7)
Sn(1)−Fe(2)	2.4612(9)	O(5)−C(11)	1.128(8)
Fe(2)−C(12)	1.761(6)	O(6)−C(12)	1.145(7)
Fe(2)−C(10)	1.773(6)	C(1)−C(2)	1.504(7)
Fe(2)−C(9)	1.782(6)	C(1)−C(4)	1.512(7)
Fe(2)−C(11)	1.796(7)	C(1)−C(3)	1.515(8)
O(1)−C(1)	1.487(5)	C(5)−C(8)	1.496(8)
O(1)−Sn(1)′	2.087(3)	C(5)−C(6)	1.521(8)
O(2)−Sn(1)−O(1)′	94.6(1)	Sn(1)′−O(1)−Sn(1)	106.2(1)
O(2)−Sn(1)−O(1)	91.8(1)	C(5)−O(2)−Sn(1)	131.3(3)
O(1)′-Sn(1)−O(1)	73.8(1)	O(1)−C(1)−C(2)	106.3(4)
O(2)−Sn(1)−Fe(2)	134.3(1)	O(1)−C(1)−C(4)	107.9(4)
O(1)′-Sn(1)−Fe(2)	123.21(8)	C(2)−C(1)−C(4)	110.8(5)
O(1)−Sn(1)−Fe(2)	120.84(9)	O(1)−C(1)−C(3)	108.2(4)
C(12)−Fe(2)−C(10)	92.6(3)	C(2)−C(1)−C(3)	112.5(4)
C(12)−Fe(2)−C(9)	91.3(3)	C(4)−C(1)−C(3)	110.9(4)
C(10)−Fe(2)−C(9)	114.9(3)	O(2)−C(5)−C(8)	108.5(5)
C(12)−Fe(2)−C(11)	89.2(3)	O(2)−C(5)−C(6)	111.3(4)
C(10)−Fe(2)−C(11)	120.7(3)	C(8)−C(5)−C(6)	110.7(6)
C(9)−Fe(2)−C(11)	124.4(3)	O(2)−C(5)−C(7)	104.0(5)
C(12)−Fe(2)−Sn(1)	174.8(2)	C(8)−C(5)−C(7)	110.4(5)
C(10)−Fe(2)−Sn(1)	92.2(2)	C(6)−C(5)−C(7)	111.6(6)
C(9)−Fe(2)−Sn(1)	88.4(2)	O(3)−C(9)−Fe(2)	177.2(5)
C(11)−Fe(2)−Sn(1)	86.7(2)	O(4)−C(10)−Fe(2)	176.0(5)
C(1)−O(1)−Sn(1)′	125.8(3)	O(5)−C(11)−Fe(2)	176.8(6)
C(1)−O(1)−Sn(1)	126.0(2)	O(6)−C(12)−Fe(2)	179.3(6)

[a] Symmetry transformations used to generate equivalent primed atoms: $-x, -y + 2, -z + 1$.

Synthesis of $[Sn(\mu\text{-}N^tBu)(\mu\text{-}NH^tBu)(SiMe_2)][Fe\{Si(OMe)_3(CO)_3(dppm\text{-}P)\}]$ (7). To a solution of $[HFe\{Si(OMe)_3(CO)_3(dppm\text{-}P)\}]$ (0.533 g, 0.82 mmol) in THF (40 mL) was added dropwise with stirring and at room temperature a solution of $Sn(\mu\text{-}N^tBu)_2SiMe_2$ (**4**; 0.21 mL, 0.82 mmol; $d = 1.25$ g/cm^3) in THF (10 mL). The brown reaction mixture rapidly turned black, and a pure solid could not be isolated. Spectroscopic data for the solution are as follows. $^{31}P\{^1H\}$ NMR (81 MHz, C_6D_6): δ −24 (d, 1 P, uncoordinated PPh_2, $^2J(P,P_{Fe}) = 85$ Hz), 74 (d, P_{Fe}). $^{119}Sn\{^1H\}$ NMR (74.68 MHz, C_6D_6): δ 496.9 (m).

Synthesis of $[(OC)_3\{(MeO)_3Si\}Fe(\mu\text{-dppm})Sn(O^tBu)]$ (8). To a solution of $[HFe\{Si(OMe)_3(CO)_3\}(dppm\text{-}P)]$ (0.200 g, 0.3 mmol) in THF (40 mL) was added dropwise with stirring at room temperature a solution of $[Sn(O^tBu)(\mu\text{-}O^tBu)]_2$ (**6**; 0.850 g, 0.32 mmol) in THF (40 mL). The reaction mixture turned from red to black. After the mixture was stirred for 3 h at room temperature, half of the solvent was removed under reduced pressure and the solution was cooled to −5 °C. After a few weeks, the product crystallized as very dark red crystals (yield 0.223 g, 90%). ^1H NMR (200.13 MHz, C_6D_6): δ 1.44 (m, 9 H, $C(CH_3)_3$), 3.57 (t, 2 H, PCH_2P), 3.81 (s, 9 H, $Si(OMe)_3$), 6.7−7.6 (m, 20 H, phenyls). $^{31}P\{^1H\}$ NMR (81 MHz, C_6D_6): δ −15.0 (m, P_{Sn}, $^{2+3}J(PP) = 132$ Hz, $^1J(P_{Sn}{}^{119}Sn) = 703$ Hz, $^1J(P_{Sn}{}^{117}Sn) = 672$ Hz), 63.0 (m, P_{Fe}, $^{2+3}J(PP) = 132$ Hz, $^2J(P_{Fe}Sn) = 61$ Hz, $^2J(P_{Fe}Si) = 24$ Hz). $^{119}Sn\{^1H\}$ NMR (74.68 MHz, C_6D_6): δ 404.5 (q, $^1J(P_{Sn}{}^{119}Sn) = 703$ Hz, $^2J(P_{Fe}Sn) = 61$ Hz). $^{29}Si\{^1H\}$ NMR (39.7 Hz, C_6D_6): δ 5.0 (q, $^2J(P_{Fe}Si) = 24$ Hz, $^3J(P_{Sn}Si) = 3$ Hz). Anal. Calcd for $C_{35}H_{40}O_7P_2SiSnFe$: C, 50.22; H, 4.78. Found: C, 50.20; H, 4.70.

Synthesis of $[Fe(CO)_4Sn(O^tBu)(\mu\text{-}O^tBu)]_2$ (9). A solution of $[Sn(O^tBu)(\mu\text{-}O^tBu)]_2$ (1.00 g, 3.77 mmol) in toluene (20 mL) was added to $[Fe_2(CO)_9]$ (1.50 g, 4.12 mmol) in toluene (50 mL) with stirring. The mixture was stirred at 70 °C for 1 h, and it rapidly turned dark green owing to the formation of $[Fe_3(CO)_{12}]$. After the mixture was cooled to room temperature, the volatiles were removed under reduced pressure. The residue was dissolved in toluene, and evaporation under reduced pressure removed the residual $[Fe(CO)_5]$. Redissolution of the brown residue in toluene (25 mL) and cooling of the solution to −5 °C afforded orange crystals of the product (yield 1.34 g, 82%). FT-IR (toluene): ν(CO) 1927 (vs), 1960 (m), 2036 (s) cm^{-1}. ^1H NMR (200.13 MHz, C_6D_6): δ 1.41 (s). $^{13}C\{^1H\}$ NMR (50.32 MHz, C_6D_6): δ 31.3 (s, 6 H, CH_3), 77.6 (s, 2 C, CMe_3), 211.9 (s, 1 CO), 212.69 (s, 3 CO). $^{119}Sn\{^1H\}$ NMR (74.68 MHz, C_6D_6): δ 36.37 (s). Anal. Calcd for $C_{24}H_{36}O_{12}Sn_2Fe_2$: C, 33.13; H, 4.16. Found: C, 33.77; H, 4.30.

X-ray Crystallography. The most relevant data for the X-ray structure analyses of single crystals of **1**, **8**, **9a**, and **9b** are collected in Table 5. While the reflection intensities for **1**, **9a**, and **9b** have been collected at room temperature on a Siemens-Stoe AED apparatus using Mo Kα ($\lambda = 0.7107$ Å) radiation, those for **8** have been obtained from an image plate Stoe IPDS instrument with the same radiation. All structures have been solved by applying heavy-atom methods.[30] In the final refinement cycles anisotropic temperature factors have been attributed to the heavy atoms (except for THF in **8**), while the hydrogen atoms have been refined with adequate geometries (methyl groups with tetrahedral angles and standard C−H distances).

Acknowledgment. We are very grateful to Dr. Ch. Stern (Strasbourg) for preliminary experiments and to the CNRS, the Ministère de l'Education Nationale, de la Recherche et de la Technologie and the Ministère des

Table 5. Crystallographic Data and Structure Refinement Details for 1, 8, 9a, and 9b

	1	8	9a	9b
formula	$C_{10}H_{19}FeN_3O_4Si$	$C_{35}H_{40}FeO_7P_2SiSn\cdot C_4H_8O$	$C_{24}H_{36}Fe_2O_{12}Sn_2$	$C_{24}H_{36}Fe_2O_{12}Sn_2$
fw	329.22	909.34	865.61	865.61
cryst syst	orthorhombic	monoclinic	triclinic	monoclinic
space group	*Pbca*	$P2_1/c$	$P\bar{1}$	$P2_1/n$
a, Å	14.112(7)	11.885(2)	8.948(2)	8.996(2)
b, Å	14.793(9)	21.256(4)	10.328(2)	11.638(2)
c, Å	15.233(10)	17.577(4)	10.866(2)	16.057(3)
α, deg	90	90	108.46(3)	90
β, deg	90	100.62(3)	91.78(3)	92.13(3)
γ, deg	90	90	115.06(3)	90
V, Å^3	3180(3)	4364.4(15)	846.8(3)	1679.9(6)
Z	8	4	1	2
ρ_{calcd}, g cm^{-3}	1.375	1.384	1.698	1.711
μ, mm^{-1}	1.035	1.051	2.349	2.368
θ range, deg	2.40−22.50	1.74−24.28	2.01−22.51	2.16−24.19
no. of rflns collected	2077	20 660	2150	2514
no. of indep rflns	2077 (R(int) = 0.0000)	6913 (R(int) = 0.1534)	2150 (R(int) = 0.0000)	2514 (R(int) = 0.0000)
final *R* indices ($I > 2\sigma(I)$)	R1 = 0.0322, wR2 = 0.0737	R1 = 0.0710, wR2 = 0.1766	R1 = 0.0261, wR2 = 0.0705	R1 = 0.0281, wR2 = 0.0745
R indices (all data)	R1 = 0.0464, wR2 = 0.0836	R1 = 0.1702, wR2 = 0.2069	R1 = 0.0265, wR2 = 0.0709	R1 = 0.0341, wR2 = 0.0799

Affaires Etrangères (Paris), the Deutsche Forschungsgemeinschaft (Bonn), and the DAAD (PROCOPE project) for support.

(30) Sheldrick, G. M. Shelx-98, Program for X-ray Structure Determination; University of Göttingen, Göttingen, Germany, 1998.

Supporting Information Available: Tables of atom parameters, anisotropic temperature factors, and all bond distances and angles. This material is available free of charge via the Internet at http://pubs.acs.org.

OM000515Z